Applied Surface Science 285P (2013) 865–873

Contents lists available at ScienceDirect

Applied Surface Science

journal homepage: www.elsevier.com/locate/apsusc

Preparation, characterization and adsorption properties of chitosan modified magnetic graphitized multi-walled carbon nanotubes for highly effective removal of a carcinogenic dye from aqueous solution

HuaYue Zhu [a,b], YongQian Fu [a], Ru Jiang [a,b,*], Jun Yao [a], Li Liu [b], YanWen Chen [a], Ling Xiao [b], GuangMing Zeng [c,**]

[a] Laboratory of Bioresource Utilization and Pollution Control, College of Life Science, Taizhou University, Taizhou 318000, Zhejiang, PR China
[b] Hubei Biomass-Resource Chemistry and Environmental Biotechnology Key Laboratory, Wuhan University, Wuhan 430072, Hubei, PR China
[c] Key Laboratory of Environmental Biology and Pollution Control, Hunan University, Ministry of Education, Changsha 410082, Hunan, PR China

ARTICLE INFO

Article history:
Received 24 June 2013
Received in revised form 31 August 2013
Accepted 1 September 2013
Available online 8 September 2013

Keywords:
Adsorption
Graphitized multi-walled carbon nanotubes
Magnetic separation
Dye
Chitosan

ABSTRACT

Novel chitosan-modified magnetic graphitized multi-walled carbon nanotubes (CS-m-GMCNTs) were synthesized via a suspension cross-linking method. Composition, morphology and magnetic properties of as-prepared CS-m-GMCNTs were characterized by XRD, SEM-EDS, BET and VSM. The large saturation magnetization (12.27 emu g^{-1}) allows fast separation of CS-m-GMCNTs from treated aqueous solution. The adsorption of congo red (CR) on CS-m-GMCNTs was strongly dependent on pH, temperature of the aqueous phase and adsorbent dosage. Up to 100 and 94.58% color removal could be achieved in 100 min contact time with 10 and 50 mg L^{-1} of initial concentrations, respectively. The adsorption capacity of CR onto CS-m-GMCNTs could reach 262.9 mg g^{-1}. The pseudo-second-order kinetic model with high correlation coefficients ($R^2 > 0.999$) was suitable to describe the process of CR adsorption onto CS-m-GMCNTs. The Langmuir model fitted the adsorption isotherm data better than the Freundlich model. Values of thermodynamic parameters (ΔG°, ΔH° and ΔS°) indicated that the adsorption process was strongly dependent on temperature of the aqueous phase, and spontaneous and endothermic process in nature. Therefore, CS-m-GMCNTs adsorbent displays main advantages of excellent dispersion, convenience separation and high adsorption capacity, which implies their potential application in the environmental cleanup.

1. Introduction

Carbon nanotubes (CNTs) have attracted special interest in interdisciplinary fields owing to their large specific surface area, highly porous and hollow structure, which has shown promising applications in many areas including environmental engineering since their discovery in 1991 by Iijima [1–4]. Recently, numerous studies have demonstrated their potential application in adsorption removal of different pollutants such as metallic ions [5,6], synthesized dye [7], and other hazardous organic compounds [8]. Generally, adsorption capacities of CNTs toward these pollutants were superior to those of activated carbon, which resulted from the stronger interactions between objective pollutants and CNTs [5]. However, some obvious obstacles of raw CNTs, such as poor dispersion in aqueous solutions, lack of surface functional groups and the difficulty in collecting them from the treated effluents greatly restricted their actual application in the removal of pollutants [9].

Recently, modification of CNTs with biopolymers has attracted significant interest due to their hydrophilicity, excel dispersion in aqueous solution and excellent adsorption properties [3,4,10–12]. It opens up new prospects for the preparation and application of novel biopolymer modified CNTs materials. Among those biopolymers used, chitosan is a kind of excellent adsorbent for the removal of dyes and metal ions in aqueous solution due to its high content of hydroxyl and amino groups in the polymer chains [13,14]. By sonication or covalent modification, chitosan and its derivatives could be grafted onto the surface of CNTs, resulting in provisionally stable suspension of CNTs in acidic or neutral aqueous solutions [4,10,15–18]. Some studies have demonstrated that the dispersion of CNTs could be dramatically improved using chitosan possibly due to a higher surface coverage of the CNTs [12,19]. Except for the excellent dispersion, chitosan/CNTs nanocomposite also possessed higher adsorption capacities for removing many kinds of organic

* Corresponding author at: No. 1139, Municipal Government Avenue, Jiaojiang District, Taizhou City, Zhejiang Province 318000, PR China. Tel.: +86 158 6763 6396; fax: +86 576 8513 7066.
** Co-corresponding author. Tel.: +86 731 8822 754; fax: +86 731 8823 701.
E-mail addresses: jiangru0576@163.com (R. Jiang), zgming@hnu.cn (G. Zeng).

0169-4332/$ – see front matter © 2013 Elsevier B.V. All rights reserved.
http://dx.doi.org/10.1016/j.apsusc.2013.09.003

and inorganic pollutants such as 4,4-dichlorobiphenyl [8], synthesized azo dye [20] and heavy metals [21]. Generally, the numerous hydroxyl and amino groups in the polymer chains of chitosan resulted in an obvious enhancement in the adsorption of pollutants on chitosan/CNTs nanocomposite. However, the difficulty in collecting these chitosan/CNTs nanocomposite from treated effluents can cause inconvenience in their practical application. Therefore, it is necessary and significant to explore novel functionalized chitosan/CNTs nanocomposite that are able to be easily separated from the treated solution except for excellent dispersion in solution and adsorption property. Recently, magnetic chitosan and magnetic carbon nanotubes for removal of pollutants from aqueous solutions have been obtained and studied since magnetic separation technique has some advantages, such as high efficiency, cost-effectiveness [5–7,22–28]. However, to the authors' knowledge, there are rarely been reported to explore the potentiality of combining these two magnetic adsorbents and using it for effective removal of a carcinogenic textile dye from aqueous environments.

Based on the above considerations, novel chitosan-modified magnetic graphitized multi-walled carbon nanotubes (CS-m-GMCNTs) were synthesized via a suspension cross-linking method and characterized by XRD, SEM-EDS, BET and VSM in this study. The obtained magnetic CS-m-GMCNTs were used as an adsorbent for effective removal of a carcinogenic textile dye, congo red (CR in chief), from aqueous solutions. The adsorption isotherm, kinetics, thermodynamics, and mechanisms involved in the adsorption process were also discussed, which would provide a theoretical foundation for further applications of system design in the sequestration or removal of hazardous pollutants.

2. Experimental

2.1. Chemicals

Graphitized multi-walled carbon nanotubes (GMCNTs in chief, purity > 99.9 wt%, diam. 15 ± 5 nm, length 10–30 μm) were purchased from Chengdu Organic Chemistry Co., Ltd., Chinese Academy of Sciences (Chengdu, China). Chitosan with 91% degree of deacetylation (DD) and 2.1×10^5 of molecular weight was purchased from Yuhuan Jinke Co., Ltd. (Taizhou, China). Congo red ($C_{32}H_{22}N_6O_6S_2Na_2$, molecular weight 696.67) used as a model carcinogenic dye was purchased from Yongjia Fine Chemical Factory (Wenzhou, China). N_2 with 99% in purity was used as protective gas from Haitian-Gas Co., Ltd. (Taizhou, China). $FeSO_4{\cdot}7H_2O$, $Fe(NO_4)_3{\cdot}9H_2O$ and other reagents of analytical grade were purchased from Shanghai Chemical Reagents Research Institute. All reagents were used without further treatment.

2.2. Preparation of Fe_3O_4 nanoparticles

Fe_3O_4 nanoparticles were prepared by co-precipitating ferric and ferrous salts in anaerobic conditions and treating under hydrothermal conditions according to the modified method [29]. Ferric and ferrous ions (molar ratio 2:1) were dissolved in deoxygenated double-distilled water at a total concentration of 0.3 M iron ions under the protection of N_2. After 30 min, the mixed solution of iron salts was added to 200 mL of chitosan-acetic acid solution (0.25 wt%) under vigorous stirring in a N_2 atmosphere. Chemical precipitation was achieved at 343 K by adding 40 mL of NH_4OH solution (29.6%, v/v) with continuously vigorous stirring. During the reaction process, the pH was maintained at about 10. The precipitates were kept at 343 K for 20 min. After the suspension was heated up to 353 K and kept for 5 h, the suspension was cooled down to room temperature and the precipitates (magnetite) were separated by magnetic decantation. Separation-redispersion cycles were carried for several time with ethanol and distilled water and then finally dried in a vacuum oven at 353 K.

2.3. Preparation of CS-m-GMCNTs

The magnetic CS-m-GMCNTs were prepared via a suspension cross-linking method. The procedure was as follows: 0.2 g chitosan was dissolved in 40 mL of acetic acid aqueous solution (2%, v/v). 0.4 g Fe_3O_4 nanoparticles and 0.4 g GMCNTs were dispersed in a solution with 80 mL paraffin and 4 mL span-80 and the mixture was mechanically stirred for 30 min. After a steady emulsion had formed, 2.0 mL of glutaraldehyde solution (25%, v/v) was added and the crosslinking reaction was allowed to proceed for 1 h at 343 K under stirring. The temperature was further increased to 353 K and the pH was adjusted to 9–10. A black product (CS-m-GMCNTs) appeared and was separated from the reaction system by a magnet and washed for three times with N,N-dimethylformamide, ethanol and distilled water, respectively. Finally, CS-m-GMCNTs were dried in an oven at 353 K under atmospheric condition.

2.4. Characterization of CS-m-GMCNTs

X-ray diffraction (XRD) measurements were performed on powdered samples in a Bruker Advance D8 X-ray diffractometer. The voltage and current used were 40 kV and 30 mA, respectively, and XRD patterns were obtained in the 2θ range of 10°–70° at 5° min^{-1} scanning speed. CS-m-GMCNTs were mounted onto stubs using a double sided adhesive tape and coated with gold. The coated samples were observed using a Hitachi SX-650 scanning electron microscope with the energy dispersive spectrometer (EDS) at the required magnification. A commercial HH-15 model vibrating sample magnetometer (VSM) (Nanjing University, China) was used at room temperature to characterize the magnetic properties of CS-m-GMCNTs. N_2 adsorption-desorption isotherms on CS-m-GMCNTs at 77 K was measured on a Micromeritics ASAP2020, from which the Brunauer–Emmett–Teller (BET) surface area and Barrett–Joyner–Halenda (BJH) pore size were calculated, respectively.

2.5. Batch adsorption studies

Batch adsorption experiments were carried out on a model KYC-1102C thermostate shaker (Ningbo, China). For a typical batch experiment, about 50 mg of CS-m-GMCNTs was incubated with 50 mL of CR solution for 3 h. At completion of predetermined time intervals, 5 mL of dispersion was drawn and CS-m-GMCNTs adsorbent was separated immediately by a magnet from treated solutions. Residual CR concentration in supernate was analyzed at λ_{max} = 496.0 nm using a Cary 50 model UV–visible spectrophotometer (Varian, USA). Adsorbed amount (q_t) of CR per unit weight of dry CS-m-GMCNTs at time t and removal efficiency (η) of CR on CS-m-GMCNTs were calculated by Eqs. (1) and (2), respectively.

$$q_t = \frac{(C_0 - C_t)V}{W} \quad (1)$$

$$\eta(\%) = \frac{C_0 - C_t}{C_0} \times 100 \quad (2)$$

where C_0 and C_t (mg L^{-1}) are the initial CR concentration and the CR concentrations at any time t (min), respectively; V (L) is the volume of the CR solution; and W (g) is the weight of CS-m-GMCNTs used.

All adsorption experiments were performed in triplicate, and the averaged values were taken and reported in this study.

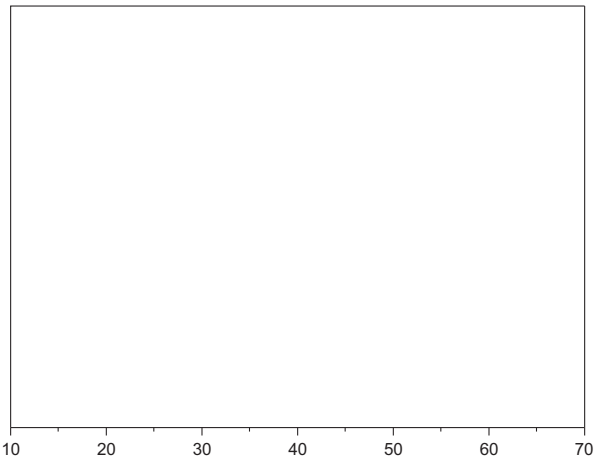
10
20
30
40
50
60
70

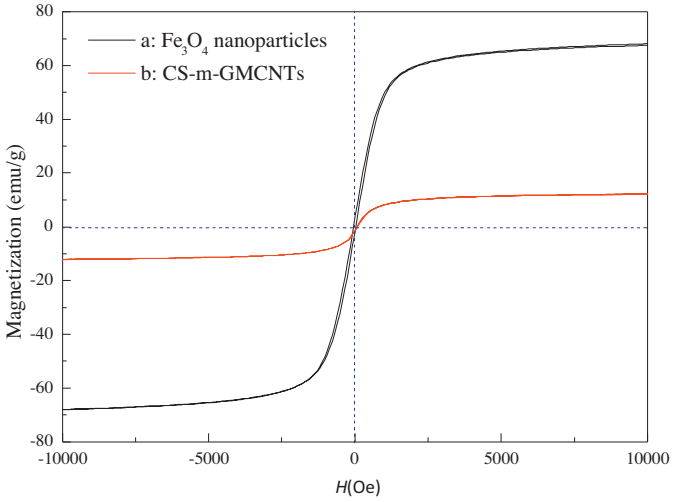

Fig. 3. Magnetic hysteresis curves of Fe_3O_4 (a) and CS-m-GMCNTs (b).

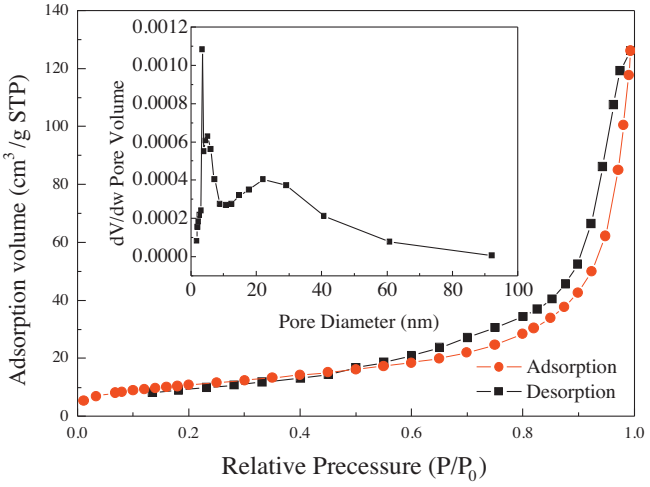

Fig. 5. BET adsorption–desorption isotherms and pore volume distribution (inset) of CS-m-GMCNTs.

CS-m-GMCNTs showed a tendency to be attracted by a permanent magnet and the CR solution turned transparent and colorless after the recycling of CS-m-GMCNTs from treated solution when a permanent magnet was placed nearby (Fig. 4(c) and (d)). Therefore, the prepared CS-m-GMCNTs adsorbent displayed the main advantages of the convenient recycling from aqueous solution and high adsorption capacity, which implied their potential application for effective removal of dye molecules and other pollutants from aqueous solution.

3.1.4. Brunauer–Emmett–Teller (BET) surface area

The BET surface area and pore structure of the as-prepared CS-m-GMCNTs have been investigated using N_2 adsorption–desorption measurements and the corresponding result is displayed in Fig. 5. The BET surface area of CS-m-GMCNTs was obtained as 39.20 $m^2\,g^{-1}$ and the total pore volume (V_P) was obtained as 0.129 $cm^3\,g^{-1}$. A great specific surface area (39.20 $m^2\,g^{-1}$) of CS-m-GMCNTs can supply more surface active sites, leading to an enhancement of adsorption performance. It is suggested that the pore structure of the adsorbent materials used consists of macropores, mesopores and micropores. Pore volume distribution of CS-m-GMCNTs was presented in Fig. 5(inset). Two major pore widths (3.4 and 22.0 nm) were detected, which indicated that CS-m-GMCNTs have a mesoporous structure and makes it easy for CR to penetrate into the mesopores of CS-m-GMCNTs.

3.2. Effect of initial CR concentration on adsorption

The initial adsorbate concentration plays an important role in the adsorption capacity of dye on adsorbent. Fig. 6 shows the effect of different initial CR concentration on color removal and adsorption capacity (q_t) of CR onto CS-m-GMCNTs. After 20 min, decolorization efficiency of CR was 97.37%, 81.47%, 72.40%, 63.65% and 54.99% when the initial concentration was 10 $mg\,L^{-1}$, 20 $mg\,L^{-1}$, 30 $mg\,L^{-1}$, 40 $mg\,L^{-1}$ and 60 $mg\,L^{-1}$, respectively. However, after 120 min, the corresponding decolorization efficiency reached to 100%, 99.28%, 99.14%, 96.97% and 94.58%, respectively. The results indicated that CS-m-GMCNTs possessed excellent adsorption property for effectively removing CR azo dye from aqueous solution. As seen in Fig. 6(b), q_t value increased evidently from 9.82 $mg\,g^{-1}$ to 58.32 $mg\,g^{-1}$ with the increase in initial concentration from 10 $mg\,L^{-1}$ to 60 $mg\,L^{-1}$. The result that adsorption capacity of CR increased with the increasing of initial CR concentration might be attributed to an increase in the driving force of a concentration gradient with the increase in the initial concentration. For CS-m-GMCNTs, some possible interactions including electrostatic interactions, hydrogen bonds, π–π bonds, covalent and hydrophobic effect are responsible for the adsorption of organic chemicals on the surface of carbon nano-sized particles.

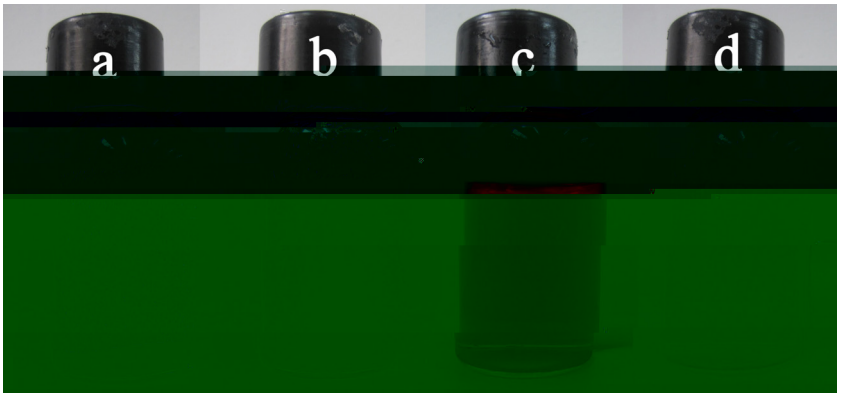

Fig. 4. Optical photographs: GMCNTs existed in aqueous solution (a), CS-m-GMCNTs dispersed in aqueous solution (b), the CR solution (c), and separation of CS-m-GMCNTs from treated CR solution by a magnet (d).

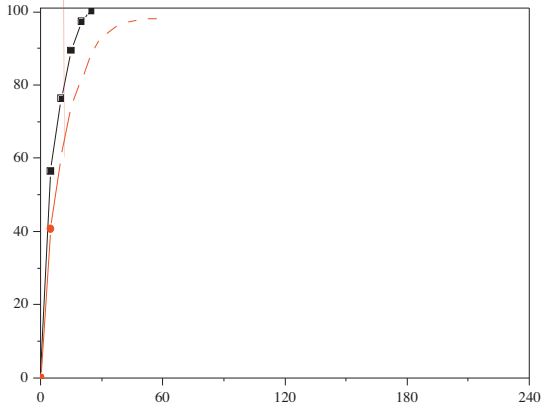
100
80
60
40
20
0
0
60
120
180
240

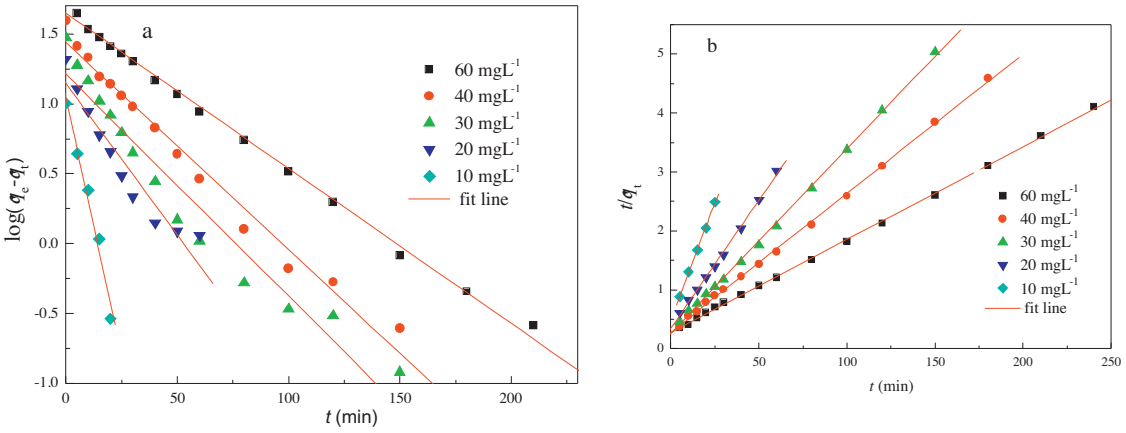

Fig. 8. First-order kinetic plots (a) and second-order kinetic plots (b) for the adsorption of CR on CS-m-GMCNTs.

Obviously, the theoretical $q_{e,cal}$ values calculated from the Lagergren-first-order kinetic model gave significantly different values compared to corresponding experimental values ($q_{e,exp}$), and the correlation coefficients ($R^2 < 0.985$) were also found to be lower (Fig. 8(a) and Table 1). These results indicated that the Lagergren-first-order kinetic model might not be sufficient to describe the adsorption process of CR on CS-m-GMCNTs. Whereas the pseudo-second-order equation showed well fit to the experimental data with higher squared correlation coefficients ($R^2 > 0.998$) (Fig. 8(b) and Table 1). The pseudo-second-order model is based on the assumption that the rate-determining step may be a chemical adsorption involving valence forces through sharing or exchange of electrons between adsorbent and adsorbate [36]. Values of k_2 decreased from 1.84×10^{-2} to 1.05×10^{-3} (g mg^{-1} min^{-1}) with the increase in CR solution from 10 mg L^{-1} to 60 mg L^{-1}. This result is further proven that adsorption of CR onto CS-m-GMCNTs increased with the increasing of initial CR concentration resulting from an increase in the driving force of a concentration gradient.

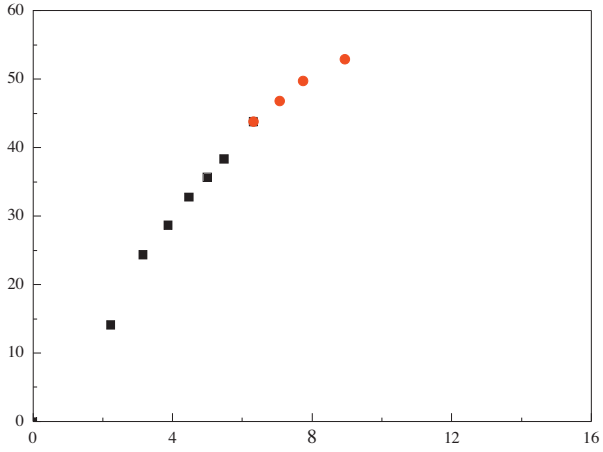

In order to investigate diffusion mechanism during adsorption of CR solution onto CS-m-GMCNTs, the intraparticle diffusion model (Eq. (6)) has also been studied. Generally, the interpretation of overall adsorption behavior in terms of the true diffusivity and equilibrium properties is not always straightforward. However, an apparent diffusion coefficient can be derived by fitting the adsorption experimental data obtained from the slope of the linear plot of q_t versus $t^{1/2}$. The plots of q_t versus $t^{1/2}$ for CR adsorption on CS-m-GMCNTs at different initial concentrations are shown in Fig. 9. The intraparticle diffusion constants (k_{id1}, k_{id2}) and the correlation coefficient (R^2) are shown in Table 2. According to Fig. 9, the adsorption of CR onto CS-m-GMCNTs went through three consecutive stages, which is typical adsorption onto mesoporous materials. It was in agreement with the above-mentioned discussion on the BET analysis. Generally, first stage is attributed to the external surface adsorption correlated to the boundary layer diffusion, which is assumed to occur rapidly and does not form a rate-limiting stage in the adsorption of organic pollutant on activated carbons. From Table 2, it can be seen that the order of adsorption rate in the first

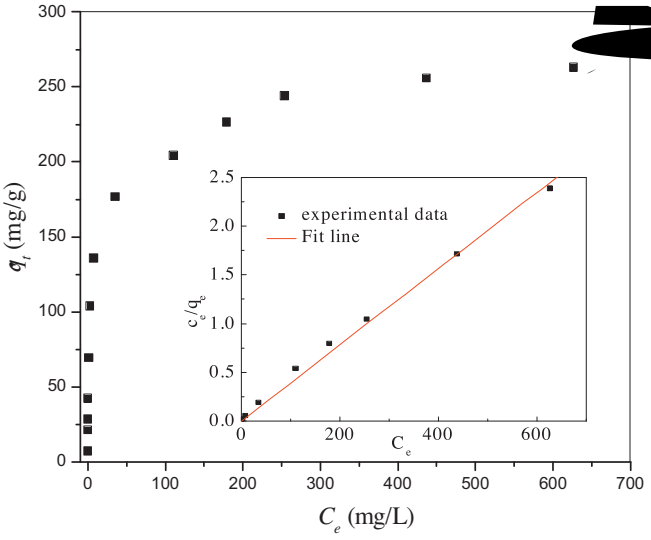

Fig. 10. Equilibrium isotherms for the adsorption of CR on CS-m-GMCNTs at 298 K. The insets illustrate the linear dependence of C_e/q_e on C_e.

important in the design of an adsorption system [37]. Adsorption experiments were conducted at 298 K to investigate the adsorption isotherm. In this work, equilibrium data for CR adsorption on CS-m-GMCNTs were modeled using the Langmuir equation (Eq. (6)) [38] and the Freundlich equation (Eq. (7)) [39]:

$$\frac{C_e}{q_e} = \frac{C_e}{q_m} + \frac{1}{K_L q_m} \tag{6}$$

$$\log\ q_e = \log K_F + \frac{1}{n} \log\ C_e \tag{7}$$

where q_m is the maximum amount of adsorption which complete monolayer coverage on the adsorbent surface (mg g^{-1}), and K_L is the Langmuir binding constant, which is related to the energy of adsorption (L mg^{-1}). C_e is the concentration of the dye solution at adsorption equilibrium (mg L^{-1}), K_F [mg g^{-1} (L g^{-1})$^{-1/n}$] and n are the Freundlich constants related to the adsorption capacity and intensity, respectively.

The results drawn from Fig. 10 and Table 3 indicated that the Langmuir model had a perfect application for CR adsorption on CS-m-GMCNTs with a regression coefficient (R^2) of 0.996 while the correlation coefficients (R^2) of Freundlich models was 0.857. In addition, the q_m value for the adsorption of CR by CS-m-GMCNTs was 261.8 mg g^{-1}, which agreed well with the experimental value $q_{e,\mathrm{exp}}$ (263.3 mg g^{-1}). Obviously, the Langmuir isotherm, compared with the Freundlich isotherm, was more suitable to describe the adsorption of CR on CS-m-GMCNTs. In other words, this adsorption process acted as monolayer adsorption on the surface of CS-m-GMCNTs under the applied exp[illegible]ital condition.

Further, a dimensionless constant, separation factor or "Langmuir parameter" (R_L), obtained from the

[27] H.Y. Zhu, Y.Q. Fu, R. Jiang, J. Yao, L. Xiao, G.M. Zeng, Novel magnetic chitosan/poly(vinyl alcohol) hydrogel beads: preparation, characterization and application for adsorption of dye from aqueous solution, Bioresour. Technol. 105 (2012) 24–30.
[28] H.Y. Zhu, R. Jiang, Y.-Q. Fu, J.H. Jiang, L. Xiaob, G.M. Zeng, Preparation, characterization and dye adsorption properties of γ-Fe_2O_3/SiO_2/chitosan composite, Appl. Surf. Sci. 258 (2011) 1337–1344.
[29] L. Liu, L. Xiao, H.Y. Zhu, Preparation and characterization of CS–Fe_3O_4@ZnS:Mn magnetic-fluorescent nanoparticles in aqueous media, Chem. Phys. Lett. 539–540 (2012) 112–117.
[30] Y.T. Shieh, Y.F. Yang, Significant improvements in mechanical property and water stability of chitosan by carbon nanotubes, Eur. Polym. J. 42 (2006) 3162–3170.
[31] J. Li, R. Hong, G. Luo, Y. Zheng, H. Li, D. Wei, An easy approach to encapsulating Fe_3O_4 nanoparticles in multiwal 0 0 4.4633 254.p6.2071693-.0002 168.6944 666.2076 Tm0 g( )Tj/F1 1 Tf6.3761 0 0 -.0761 170.4867 666.2076 Tm0 .502 .675 rg(carbon)Tj/F2 1 T